Machine Vision used in Indusries

R. Aravindhan[1] T. Ramanathan[2].

***Abstract*--Tool wear measurement is of great concern in machining industry, as it affects the surface qualities, dimensional accuracy and production costs of the machined components. The orthodox methods of measuring tool wear are time consuming and limited in accuracy and application. In this study, machine vision system based on digital image processing was developed for measurement of tool wear. The basic components of the system are: a charge coupled device (CCD) camera, PC, Microsoft Windows Video Maker, frame grabber, Video to USB cable, digital image processing software (Photoshop and digital image processing toolbox for MATLAB), multi-directional insert fixture, and light source. Tool wear images were captured and ten different wear features: length, width, area, equivalent diameter, centroid, major axis length, minor axis length, solidity, eccentricity and orientation were extracted from the images. The pixels dimension of the system was found to be *P*BB*x*BB = 0.03306 and *P*BB*y*BB = 0.03333. The accuracy of the system compared to SANDVIK CoromantPP PPhand-held microscopic lens was found to have an absolute error less than 3.13%. The system has been applied in the analysis of tool wear of uncoated cemented carbide inserts used for turning of NST 37.2 steel. A tool wear index (TWI) was proposed as a potential indicator for tool wear monitoring. A graphical user interface (GUI) was designed for easy application of system.**

Keywords: **machine vision, tool wear measurement, carbide insert, NST 37.2 steel, turning operation.**

1. INTRODUCTION

Measurement of cutting tool wear is of great concern in metal cutting operations because tool wear affects the surface qualities and dimensional accuracy of the machined components [1]. The purpose of machining is to create an acceptable surface finish within tolerance but one major problem posed by the requirement to ensure high machine utilization is the ability to correctly classify the wear state of the cutting tool [2, 3]. To ensure proper representation, cutting tools must be periodically checked and the wear measured for possible or premature failures [4]. It is also necessary to record the cutting history for a tool utilization in order to determine whether or not a tool can be safely and continuously used for a more reliable and accurate control of the machined part.

The growing demand of industrial automation in the manufacturing industry has revealed the importance of machine vision in quality inspection and process monitoring [5]. Application of machine vision systems in industry for tool wear inspection and monitoring has been of great interest in the past several years.

Several techniques have been developed for monitoring of wear state, which include indirect method such as empirical formulae, and direct method such as Toolmaker microscope or graduated magnifying lens. These orthodox methods are cumbersome, time consuming and could be inadequate. They are also limited in application because they can only be implemented off-line. The applications of image analysis (vision systems) have proved to be very efficient for area detection [4]. Bradley and Wong [6] carried out experiment using a machine vision based on sensor system. The degree of tool wear was estimated by extracting three parameters (intensity histogram, image frequency domain content and spatial domain surface texture). It was shown that tool wear can be characterized with these features. Yongjin and Fischer [7] analysed wear surface areas and material loss from the tool using micro-optics CCD monochrome camera and image processing algorithms. They were able to develop a wear index to represent tool wear condition, a control model for the machined surface, a tool life model, extended use of worn out tool and an optimal control strategy to minimize production cost in machining operation. Bahr and Motavalli [8] focused their efforts on multi-sensory tool monitoring system using vision system and vibration sensors. They combined an indirect tool monitoring technique, vibration monitoring with a direct visual monitoring technique. The vibration signals from the tool were monitored on-line using a piezoelectric accelerometer mounted on the tool holder and the tool condition is monitored periodically using a vision sensory system. The developed image processing algorithm uses neural network mathematics to measure the tool wear in the captured images. The inputs to the neural network are a set of vectors defining the characteristics of the tool surface such as surface curvature. Features such as area, perimeter, width and height of the worn area are measured to identify the extent of the tool wear. Dawson and Thomas [9] described relevant topics related to tool wear morning using wear images. He developed an automatic system for tool wear measurement. Ravindra and Srinivasa [10] elaborated on the necessity to develop a technique of quantitative tool wear measurement to determine the precise timing for tool replacement. They suggested a reliable technique for the reduction of error components by developing a system using a CCD camera to be able to precisely measure the size of tool wear in a direct manner.

From the above observations on tool wear measurements, it is clear that no single method based on the image analyses approach is available to estimate wear images over a broad range of manufacturing processes. In this work, it is desired to extract different image features from the wear surface, measure the wear, identify which measurements from the image features has the most significant effects as the wear area progresses during machining and develop a wear index that would accurately represent wear conditions as cutting progresses.

2. MATERIALS AND METHODS

Development of the vision system

The basic components of the vision system are: a CCD camera (Canon ZR 320 model with a 4.8M pixels resolution) connected with a video to USB cable to a Dell inspiron-6000 PC® with 1.5GHz processor and 1.2M bites RAM. Microsoft® Window® Video Maker version 5.1 having a 640 by 480 pixels resolution was used for the recording of the digital images, while a frame grabbing function available on the Video Maker software was used for capturing different frames (static images) from the video. Image processing software which includes: Photoshop® and digital image processing toolbox for MATLAB® were used for the analysis of the captured images.

The cutting tool insert was held in multi-directional insert fixture, which allows the insert to be turned in different directions. Two perpendicular views of the insert corresponding to the nose and flank of the insert were captured. Two incandescent light sources inclined at 45^0 to the horizontal were used to illuminate the inserts. In order to avoid background noise and interference the system was set up in a darkroom. The schematic diagram of the vision system is shown in Figure-1.

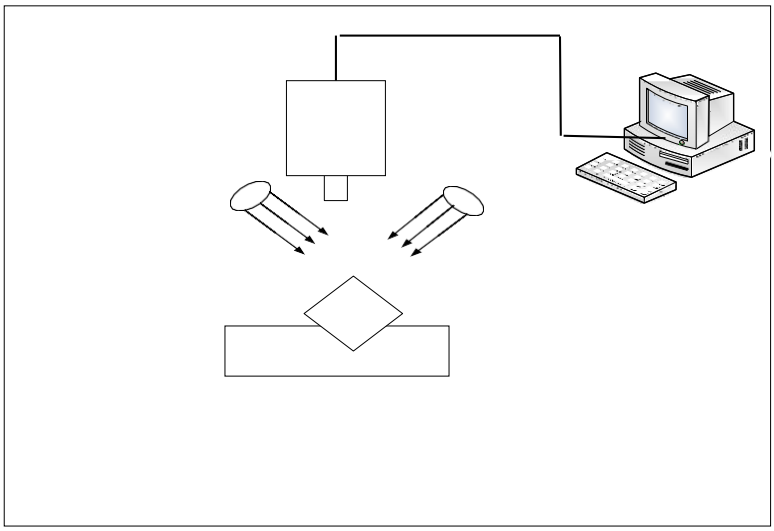

Figure-1. Schematic diagram of the vision system for measurement of tool wear.

To ensure proper accuracy in the measurements, the cutting insert was positioned parallel to the image sensor of the camera at constant distance. The Wiener filter algorithm in digital image processing toolbox for MATLAB® version 6.5 with 5x5 kernels was used for removal of background noise and image burring. To enhance the good quality of the image, a self developed shadow removing algorithm written in MATLAB® and the Canny edge detection algorithm in digital image processing toolbox for MATLAB® was used for the segmentation of the wear area in the captured image. The Canny edge detection algorithm was preferred over other edge detection methods because of its double thresholds feature that allows detection of both strong and weak edges. The detected weak edges are included in the output only if they are connected to strong edges. The captured image is then saved in 'jpeg' format for further processing.

Calibration of the vision system

For accurate dimensional measurement of the capture image, the image of the vision system was calibrated using the method proposed by Yongjin and Fischer [7]. A block of known dimensions (12 by 4.5 mm) was positioned at the same distance from the camera as the insert. The captured image of the block was analysed and the corresponding number of pixels in the x and y directions of the image of the block were counted, from which the dimensional sizes of the pixels in both x and y directions were determined as:

$$P_x = \frac{\text{dimension of block in x direction}}{\text{number of pixels in x direction}} \quad (1)$$

$$P_y = \frac{\text{dimension of block in y direction}}{\text{number of pixels in y direction}} \quad (2)$$

Where P_x and P_y are the pixel dimensions in x and y direction respectively.

Extraction of features from the captured image

2.3.1 Wear land length

The number of pixels in the segmented wear land perpendicular to cutting edge was counted using pixel counting algorithm available in the digital image processing toolbox for MATLAB®. The wear land length was computed as:

$$V_x \text{ mm} = \left\{ \sum_{i=1}^{n} P_i \right\} P_x \quad (3)$$

Where, V_x is the wear land length, $\sum_{i=1}^{n} P_i$ is total number of pixels perpendicular to cutting edge.

2.3.2 Wear land width

The number of pixels in the segmented wear land parallel to cutting edge was counted and the wear land width was computed as:

$$V_y \text{ mm} = \left\{ \sum_{k=1}^{n} P_k \right\} P_y \quad (4)$$

Where, V_y is the wear land width, $\sum_{k=1}^{n} P_k$ is total number of pixels parallel to cutting edge.

2.3.3 Wear land area

The number of pixels within the segmented area of the image was counted using pixel counting algorithm available in the digital image processing toolbox for MATLAB®. The wear area was computed as:

$$Aw \text{ mm}^2 = \left\{ \sum_{j=1}^{n} P_j \right\} P_x P_y \quad (5)$$

Where, Aw is the wear area, $\sum_{j=1}^{n} P_j$ is total number of pixels in wear areas,

2.3.4 Equivalent diameter

The equivalent diameter is defined as the diameter of a spherical particle which will give identical geometric, optical, electrical or aerodynamic behavior to that of the non spherical particle. It was computed as:

$$E_m = \sqrt{4 \left[\left(\sum_{j=1}^{n} P_j \right) P_x P_y \right] / \pi} \quad (6)$$

Where, E_m is the equivalent diameter (mm) P_y = calibrated pixels height (mm), P_j = total number of pixels in wear areas

2.3.5 Center of mass

The center of mass for the wear land area was computed using the equation developed by Yongjin et al. [1]:

$$CM_{fk} = \frac{1}{N_{fk}} \sum_{n=1}^{N_{fak}} \left[\frac{Y_{fak} + Y_{fbk}}{2} \right] \quad (7)$$

where, CM_{fk} is the Y- component in (mm) of the center of mass of the wear land area ,N_{fk} is the total number of pixels columns in the wear land area, Y_{fok} and Y_{fk} are the top and bottom Y- coordinate points of the pixel columns in wear land area,

Solidity

The solidity of the segmented wear land area was computed as the ratio of the area of the segmented area and the area of the smallest convex polygon that can contain the segmented area. It was computed as:

$$Sol = \frac{\text{number of pixels in the segmented region}}{\text{number of pixels of the smallest convex polygon that can contain the segmented region}} \quad (8)$$

Major axis length

The major axis length (x_{major}) of the segmented area was measured as the length of the major axis of the ellipse that has the same normalized second central moments as the segmented area.

2.3.8 Minor Axis Length

The minor axis length (x_{minor}) of the segmented region was measured as the length of the minor axis of the ellipse that has the same normalized

2.3.9 Eccentricity

The eccentricity (ζ) of the segmented region was measured as the ratio of the distance between the foci of the ellipse that has the same second-moments as the region and its major axis length. The value is between 0 and 1. (0 and 1 are degenerate cases; an ellipse whose eccentricity is 0 is actually a circle, while an ellipse whose eccentricity is 1 is a line segment.)

axis of the ellipse that has the same second-moments as the region.

2.4 Sensitivity analysis of the vision system

The accuracy of the proposed vision system was determined by comparing the measured values for wear region length using SANDVIK Coromant® hand-held microscopic lens (magnification = 8x) and the measured values using the vision system and the error analysis of the data was performed using the following equation:

$$error = \left| \frac{(measured-value-by-lens)-(measured-value-by-vision-system)}{measured-value-by-lens} \right| 100\% \quad (9)$$

3. RESULTS AND DISCUSSIONS

3.1 Calibration of the vision system

The image of a block with known dimensions (12 X 4.5 mm) was captured and analysed. The number of pixels along the X and Y axis of the block was counted to be 135 and 363 respectively. The dimensions of the pixel in X and Y directions were determined from Eqns 1 and 2 to be P_x = 0.03305785 mm and P_y = 0.03333333 mm. The aspect ratio of the pixel was calculated as P_x/P_y= 0.03305785/0.03333333 = 1: 1.008333, thus indicating that the dimension of the pixel is close to being a square.

Analysis of wear image using the vision system

A typical wear region on the nose of a carbide insert captured using the vision system is depicted in Figure-2. The white patch region shows the segmented wear area of the insert, while the remaining dark region shows the remaining part of the flank face of the insert. Ten different wear features: length, width, area, equivalent diameter, centroid, major axis length, minor axis length, solidity, eccentricity and orientation were extracted from the image.

Figure-2. A typical wear land on the nose of a carbide insert captured with the vision system.

Sensitivity of the vision system

The accuracy of measurements taken by the vision system compared with the measurements taken using the graduated SANDVIK Coromant® hand-held microscopic lens (magnification of 8x) for 32 random measurements of flank wear length is detailed in Table-1. The analysis showed the average absolute error was determined to be 3.13%. Thus, suggesting a high reliability of measurements taken with vision system.

3.4 Design of a graphical user interface (GUI)

A graphical user interface (GUI), was designed using the GUI toolbox for MATLAB for ease of application of the vision system. The GUI is divided into parts: input, and output section. The input section consists of a field text where the file name of the captured image to be analysed is entered. On pressing the 'get image' button, the captured wear image is loaded to the graphic window and the file name is also displayed on the window. The pixel dimensions in x and y axis are also entered in the numeric field box. In this case, the pixel dimensions in x-axis, P_x = 0.03333, and in y-axis, P_y = 0.03306. The image is analysed and the different features are extracted by pressing the 'analyse' button. The number of pixels for the wear area, equivalent diameter, centroid, major axis length, minor axis length, solidity, eccentricity and orientation are displayed in the different designated numeric field box, while the corresponding equivalent measurements in millimeter for wear area, height of wear area, width of wear area, equivalent diameter, and centroid are displayed in the different designated numeric field box. An illustrative example is shown in Figure-3 for typical wear image on carbide insert captured using the machine vision system with the file name 'c11.4fp.jpg'. The pixel dimensions in x-axis, P_x = 0.03333, and in y-axis, P_y = 0.03306 were entered. For this image, the extracted features were: wear area (693 pixels), equivalent diameter (29.7045 pixels), centroid (55,159 pixels), major axis length (43.6918 pixels), minor axis length (22.6773 pixels), solidity (8), eccentricity (0.85457) and orientation (-6.74030).

Table-1. Comparison between toolmaker's microscopic lens and vision system for measurement of flank length.

S. No.	Microscopic lens (mm)	Vision system (mm)	Absolute Error (mm)	Absolute Error %
1	0.1	0.11243	0.01242	0.6610
2	0.2	0.24687	0.04686	2.4930
3	0.3	0.27174	0.02825	1.5031
4	0.4	0.38083	0.01917	1.0199
5	0.2	0.38083	0.18082	9.6184
6	0.5	0.39883	0.10117	5.3816
7	0.6	0.42328	0.17671	9.3996
8	0.6	0.54113	0.05887	3.1314
9	0.1	0.05840	0.04159	2.2128
10	0.3	0.22223	0.07776	4.1362
11	0.4	0.26401	0.13598	7.2331
12	0.3	0.26401	0.03598	1.9139
13	0.3	0.29948	0.00051	0.0276
14	0.4	0.33413	0.06586	3.5035
15	0.4	0.38210	0.01789	0.9518
16	0.5	0.43745	0.06255	3.3271
17	0.1	0.14197	0.04197	2.2328
18	0.3	0.15329	0.14671	7.8038
19	0.3	0.25491	0.04508	2.3979
20	0.3	0.27113	0.02886	1.5355
21	0.2	0.28348	0.08348	4.4404
22	0.2	0.28632	0.08632	4.5916
23	0.4	0.38134	0.01866	0.9923
24	0.3	0.38425	0.08426	4.4817
25	0.1	0.20815	0.10815	5.7527
26	0.2	0.26025	0.06026	3.2052
27	0.4	0.36900	0.03099	1.6488
28	0.4	0.42468	0.02469	1.3132
29	0.5	0.46857	0.03142	1.6713
30	0.5	0.50796	0.00796	0.4236
31	0.6	0.58820	0.01180	0.6277
32	0.6	0.61015	0.01015	0.5396

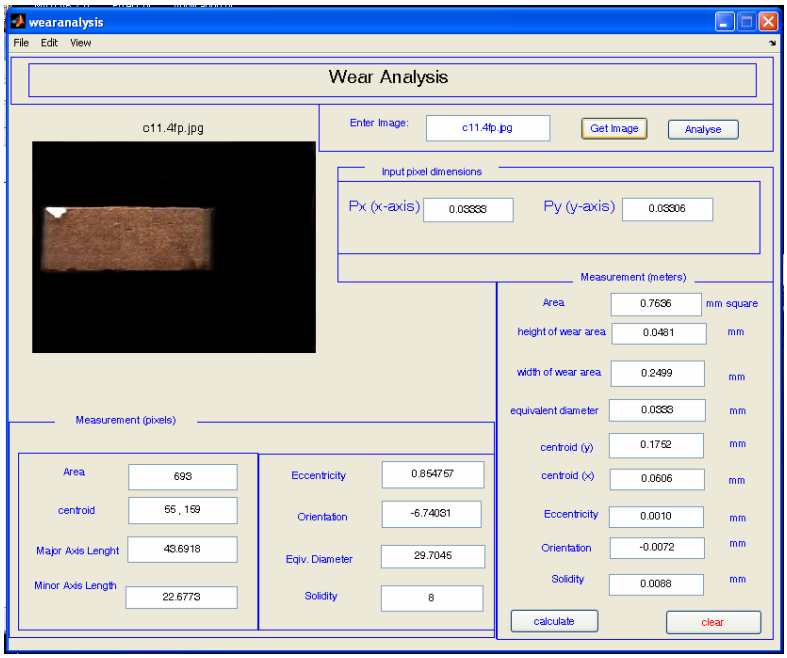

Figure-3. Graphical user interface for analysis wear image using the machine vision system.

3.5 Application of the machine vision system

The proposed machine vision system was applied in the analysis of tool wear of uncoated carbide tool insert used for typical turning operations. The turning operations were carried out on Harrison M300 lathe with spindle speed and feed rate ranging from 40-2500rpm and 0.1-1.0 mm/rev respectively. The lathe was driven by a 2.2 kW (3 hp), 3 phase, 1500 rpm motor. NST 37.2 steel bar, a commercial grade steel commonly used for production of machine components, obtained from Delta Steel Company (DSC), Ovian-Aladja, Nigeria was used as workpiece for the turning operations. SANDVIK Coromant uncoated carbide tool inserts with ISO designation SNMA 120408 was used for turning operations. The clamped geometries of the insert were: 75^0, approach angle, -6^0, side rake angle, -6^0, back rake angle, and 6^0, clearance angle. The range of cutting parameters used were: feed rate (F) = 1.0 - 2.2 mm/rev, cutting speed (CS) = 20.42-42.42 mm/s, and depth of cut (DOC) = 0.2 - 1.8 mm. Eight (8) passes of 50 mm length of cut were taken for each combination of the cutting parameters. Each cutting was carried out without the application of coolant. The wear image of the cutting tool was captured and analysed after each pass for each cutting condition.

3.6 Effect of cutting conditions on tool wear parameters

The effect of cutting conditions on the wear area, width of wear area, equivalent diameter, and centroid for both flank and nose wear are shown in Figures-4 to 7. Figure-4 shows the variations in the length (height) and width of wear area on both flank and nose with respect to number of pass for a typical cutting condition with cutting speed = 2.42 mm/s, feed rate = 0.4 mm/rev, and depth of cut = 0.2 mm. It can be seen that, (Figure-4) the wear areas expanded horizontally (length) on the tool flank and nose with increase in number of pass. Vertical expansion of the wear area occurred rather slowly (Figure-4). For this cutting condition, the nose wear was prominent than flank wear. However, as the depth of cut was increased, at values greater than the nose radius of the insert (0.8 mm), the flank wear area became much bigger than the nose wear area (not shown). The variations in wear area on the flank and nose with respect to number of pass for cutting condition with cutting speed = 29.06 mm/s, feed rate = 0.4 mm/rev, and depth of cut = 0.6 mm are shown in Figure-5. Both flank and nose progressed almost linearly with number of pass. The nose wear was consistently higher than the flank wear. This was because the depth of cut (0.6 mm) was less than the nose radius of the insert (0.8 mm).

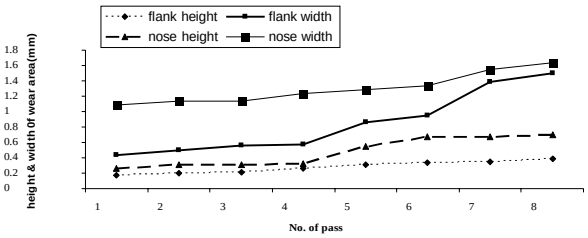

Figure-4. The variations in the height and width of wear area on the flank and nose of the insert (CS = 2.42 mm/s, F = 0.4 mm/rev, DOC = 0.2 mm).

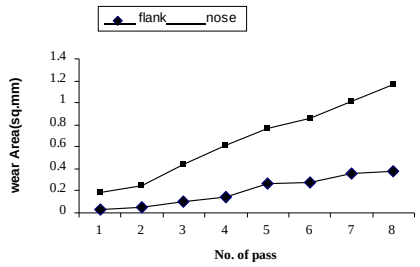

Figure-5. The variations in wear area on the flank and nose of the insert (CS = 29.06 mm/s, F = 0.4 mm/rev, DOC= 0.6 mm).

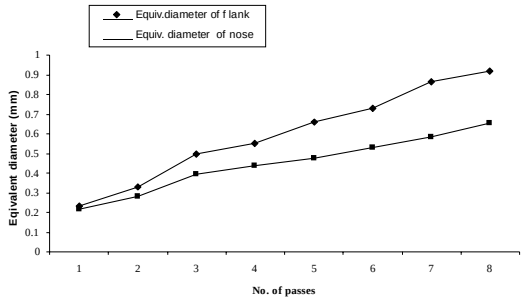

Figure-6. The variations in equivalent diameter of wear area on flank and nose of the insert (CS = 29.06 mm/s, F = 0.2 mm/rev, DOC = 1.0 mm).

The variations in equivalent diameter and the Y-component of centroid of the wear area on both flank and nose of the insert for higher values of depth of cut greater than the nose radius of the tool insert are shown in Figures-6 and 7. The equivalent diameter (Figure-6) and the centroid (Figure-7) for both flank and nose wear areas increased almost linearly with increase in number of pass. For these cutting conditions, the equivalent diameter and the Y-component of centroid of the flank wear area were consistently higher than that of the nose wear.

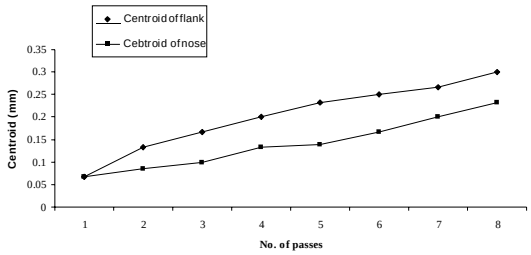

Figure-7. The variations in centroid of wear area on flank and nose of the insert (CS = 20.42 mm/s, F = 0.8 mm/rev, DOC = 2.2 mm).

3.7 Development of tool wear index (TWI)

The analysis of the wear images has shown that wear area, length and width of wear region, equivalent diameter and the Y-component of the centroid of the wear region increased steadily with increase in number of pass, thus indicating these wear parameters as potential indicators for tool wear condition monitoring. A tool wear index (TWI) to represent the overall tool wear indicator was developed by evaluating and correlating several relationships of these parameters with number of pass. The relationship (Equation 10) with the highest coefficient of determination (R^2-value) was selected as the TWI for turning of NST 37.2 steel with uncoated carbide inserts

$$TWI = \frac{Aw_f + (Aw_f)^2 + (Aw_n)^2}{(Em_f)^2 + (Em_n)^2} \quad (10)$$

Where Aw_f is the wear area on the flank, Aw_n is wear area on the nose, Em_f is the equivalent diameter of flank wear, and Em_n is the equivalent diameter of nose wear.

Table-2 shows the number of pass, area, equivalent diameter, and Y-component of centroid for both flank and nose wear areas and the computed TWI for cutting condition with cutting speed = 29.06 mm/s, feed rate = 0.8 mm/rev, and depth of cut = 1.8 mm.

Table-2. Measured features from the wear area (CS = 29.06mm/s, F = 0.8mm/rev, DOC = 1.8mm).

No. of pass	Flank wear			Nose wear			TWI
	Area (mm^2)	Equivalent diameter (mm)	Centroid (mm)	Area (mm^2)	Equivalent diameter (mm)	Centroid (mm)	
1	0.2777	0.5922	0.0333	0.2667	0.5803	0.0667	0.00029
2	0.3669	0.6807	0.1000	0.4176	0.7262	0.1333	0.00061
3	0.5465	0.8308	0.1333	0.5344	0.8215	0.1389	0.00115
4	0.6523	0.9077	0.1667	0.6247	0.8883	0.1667	0.00161
5	0.7625	0.9813	0.1791	0.633	0.8883	0.2000	0.00191
6	0.8595	0.9813	0.2195	0.8485	1.0352	0.2333	0.00271
7	0.9917	1.1191	0.2333	0.9124	1.1504	0.2999	0.00382
8	1.0391	1.1455	0.2666	0.9917	1.1726	0.3333	0.00425

Figure-8 shows the variation in TWI with the number of pass. The TWI increased exponentially with the number of pass with high coefficient of determination (R^2-value = 9889), thus indicating the high reliability of the proposed TWI as potential tool wear monitoring indicator.

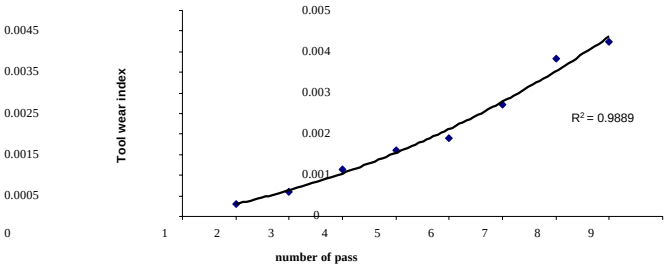

Figure-8. Variation in tool wear index (TWI) with number of pass (CS = 29.06 mm/s, F = 0.8 mm/rev, DOC = 1.8 mm).

4. CONCLUSIONS

In this paper, the development and application of a machine vision system for analysis of tool wear is described. The system consisted of a charge coupled device (CCD) camera, PC, Microsoft Windows Video Maker, frame grabber, Video/USB cable, digital image processing software (Photoshop and digital image processing toolbox for MATLAB), multi-directional insert fixture, and two light sources. Ten wear features: length, width, area, equivalent diameter, centroid, major axis length, minor axis length, solidity, eccentricity and orientation were extracted from the wear images. The system has been applied in the analysis tool wear for uncoated carbide inserts used for turning of NST 37.2 steel. The length, width, area of wear region, equivalent diameter, Y-component of centroid of wear region increased with number of pass for both flank and nose wear. The wear parameters for nose wear were consistently higher than that of flank wear for depth of cut lower than the nose radius of the insert. At depth of cut greater that the nose radius, flank wear parameters were consistently higher than that of nose wear. A tool wear index (TWI) was developed based on the extracted features The TWI increased exponentially with the number of pass with high coefficient of determination (R^2-value = 9889). Thus, indicating the suitability of the proposed TWI as a better indicator for monitoring of tool wear. Although the analysis was for uncoated carbide tool inserts used in turning operation, the system can be applied to any cutting tool and for any machining operation.

REFERENCES

[1] Kurada S. and C. Bradley. 1997. A Review of Machine Vision Sensors for Tool Condition Monitoring. Computers in Industry. 34: 55-72.

[2] Oni A.O. 2007. Development of a Machine Vision System for Measurement of Tool Wear and Surface Roughness. Unpublished M.Sc. Dissertation, University of Ibadan, Nigeria.

[3] Priya P. and B. Ramamoorthy. 2007. The Influence of Component Inclination on Surface Finish Evaluation Using Digital Image Processing. International Journal of Machine Tools and Manufacture. 47: 570-579.

[4] Al-Kindi G.A., R.M. Baul and K.F. Gill. 1992. An Application of Machine Vision in the Automated Inspection of Engineering Surfaces. International Journal of Production Research. 30(2): 241-253.

[5] Rajneesh K., P. Kulashekar, B. Dhanasekar and B. Ramamoorthy. 2005. Application of Digital Image Magnification for Surface Roughness Evaluation Using Machine Vision. International Journal of Machine Tools and Manufacture. 45: 228-234.

[6] Bradley C. and Y.S. Wong. 2001. Surface Texture Indicators of Tool Wear-A Machine Vision Approach. The International Journal of Advance Manufacturing Technology. 17: 435-443.

[7] Yongjin K. and G.W. Fischer. 2003. A Novel Approach to Quantifying Tool Wear and Tool Life Measurement for Optimal Tool Management. International Journal of Machine Tools and Manufacture 43: 359-368.

[8] Bahr B. and T. Motavalli. 1997. Sensor Fusion for Monitoring Machine Tool Conditions. International Journal of Computer Integrated Manufacturing. 10: 314-323.

[9] Dawson T. G. and R.K. Thomas. 2002. Tool life, Wear Rates and Surface Quality in Hard Turning. The George W. Woodruff school of Mechanical Engineering, Georgia Institute of Technology.

[10] Ravindra H.V. and K.R. Srinivasa. 1993. Modelling of Tool Wear Based on Cutting Forces in Turning. Indian Institute of Technology, Madras. 169(1): 25- 32.